# Load Testing and Damage Analysis of Reinforced Pre-stressed Concrete Continuous Box Girder Bridge

Gen Wang[*]

School of Construction Engineering, Jilin University, 130000 Changchun, China

[*] Correspondence: Gen Wang (aredbaddragon@outlook.com)

**Abstract:** Pre-stressed concrete continuous box girder bridges are widely used in bridge engineering due to their excellent mechanical properties. However, as the service life of the bridge increases and heavy vehicles exert additional loads, cracks may develop in the structure, leading to pre-stress loss and affecting its safety. This paper focuses on the reinforcement of an actual bridge and determines the pre-reinforcement stress state and stiffness degradation through load testing. The test results are combined with numerical simulations to analyze the stiffness of the box girder section. When the section stiffness is reduced by 5%, the deflection at the mid-span control section of the box girder is 11.7 mm, which is in good agreement with the actual condition. By integrating the bridge's appearance inspection results with numerical simulations, pre-stress loss in the box girder is analyzed. When the pre-stress loss reaches 10%, transverse cracks appear at the bottom of the main girder, similar to the results of field inspections. Based on this, the analysis considers a 5% stiffness reduction and a 10% pre-stress loss to evaluate the box girder.

## 1 Introduction

Bridges, as important infrastructure, are crucial links for urban communication. In the past three decades, China has made significant achievements in bridge construction, with the construction of a large number of new bridges providing strong support for transportation [1]. However, as the service life of bridges increases, many face issues such as material aging, environmental corrosion, and overload, leading to a gradual deterioration in performance and an inability to meet the expected load-bearing capacity [2]. Currently, the reduction in bridge load-bearing capacity and structural damage is often the result of multiple factors, including concrete aging, steel bar corrosion, and pre-stress tendon degradation [3, 4]. Therefore, to avoid potential tragedies, it is essential to effectively inspect, assess, and take necessary reinforcement measures for existing bridges [5].

Traditional reinforcement methods for existing bridges include the section enlargement method and external bonding steel method. The section enlargement method involves increasing the cross-sectional area of the beam using original materials, enhancing the effective height and reinforcement ratio of the section, thereby improving the bearing capacity and stiffness. Due to its clear stress mechanism, simple construction, and low cost, it is widely applied in the reinforcement of medium and small section beam bridges. However, the disadvantages include longer wet construction times, the need for traffic closure during the process, and a significant increase in self-weight after reinforcement, which affects the clearance of the bridge. The external bonding steel method, used when the structure cracks, involves bonding steel plates to concrete at stressed areas with adhesives or anchors, forming a strong unit that enhances the bending load-bearing capacity [6]. Its advantages include fast construction, no harm to the structure and components, and minimal impact on bridge traffic. However, the steel plates and anchors used in reinforcement need rust-proofing and rust-removal treatment, which increases maintenance and repair costs later [7–10].

Against this background, external pre-stress reinforcement technology, as an economical and effective reinforcement method, has started to be widely applied [11–13]. After the 1980s, due to the increasing durability of external pre-stress steel tendons, many countries began to apply this technology in the construction of new bridges and the reinforcement of old bridges, such as the Ponsan Bridge, Boivre, Gazde Elevated Bridge, California Long Kye Bridge, and Shingansen Sekimogawa Bridge [14–16]. Harajli et al. [17] and Vrablik et al. [18], and others studied the

strength design parameters of concrete beams after applying external pre-stress. Park et al. [19] carried out external pre-stress reinforcement on long-term operational bridges, through on-site load testing, numerical simulation, and long-term monitoring of external tendon stress loss. The results showed that external pre-stress reinforcement can effectively reduce structural deflection, and the long-term stress loss of external tendons can be neglected. Ghallab et al. [20] conducted loading tests on multiple concrete beams reinforced with external pre-stress, and the results showed that external pre-stress can increase the ultimate load-bearing capacity of the reinforced beams by approximately 75%. In summary, external pre-stress reinforcement technology can effectively improve the structural performance of bridges [21] and extend their service life. This technology applies pre-stress externally to adjust the stress state of the bridge, significantly enhancing its load-bearing capacity [22], reducing mid-span deflection, and effectively mitigating risks such as crack formation and ongoing deflection [23, 24].

## 2 Load Testing of Damaged Box Girder Before Reinforcement

This study is based on a 30+47+30m continuous box girder bridge. The bridge superstructure adopts a variable-section single-box double-chamber section. The beam height at the centerline of the box girder at the mid-span is 1.6m, while at the center pier it is 2.7m, varying according to a parabolic curve in between. The top slab and web of the box girder are segmented variable sections, with a top slab thickness of 0.25m, increasing to 0.4m at the pier top; the web is 0.35m thick within a 10.0m range at mid-span, increasing to 0.70m at the center pier, with linear variation in between, over a span of 12.0m. The thickness of the bottom slab is 0.25m within the mid-span range, increasing to 0.50m at the pier root, with a parabolic variation between these points. The section at the pier top is a solid section of 2.0m. The cross-section of the main girder is shown in Figure 1.
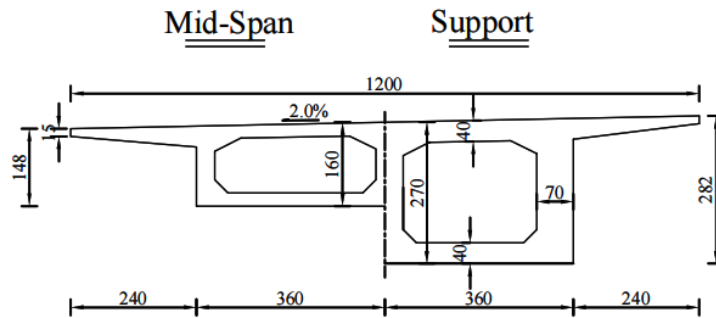


**Figure 1.** Cross-section of the main girder

According to the bridge inspection test, it was found that there were multiple stress-induced cracks in the bridge, mainly lateral cracks in the box girder. This was mainly due to insufficient effective pre-stress in the bottom slab of the box girder, causing tensile stress in the concrete at the bottom, which exceeded the tensile strength of the concrete, leading to lateral cracking. The diagonal cracks at the beam ends were primarily due to the combined effects of pre-stress, shrinkage of the web, and wing slabs in the negative bending moment region of the continuous girder.

Due to the reduction in section capacity, stiffness degradation, and other issues caused by the cracks in the bridge, it is necessary to perform structural analysis to calculate the section stress and deformation response under various working conditions. This analysis helps to infer the current stress state of the bridge structure and quantitatively evaluate the bridge's condition. Therefore, load testing was performed before the reinforcement of the bridge to determine the damage state and pre-stress loss in the 30+47+30m box girder, providing a basis for pre-stress reinforcement of the bridge structure.
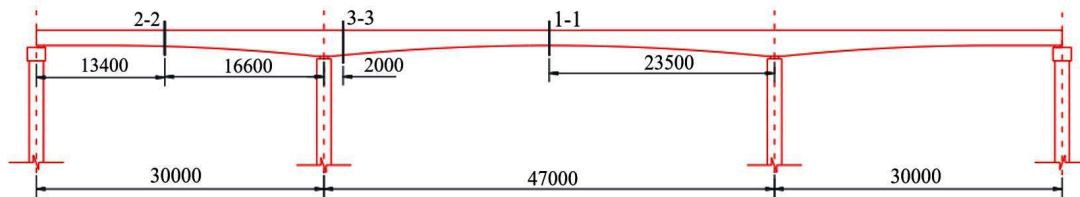


**Figure 2.** Schematic diagram of test sections (Unit: mm)

Strain and deflection measurements were taken at the mid-span sections of the side span and middle span box girders, as well as strain measurements at the upper section of the box girder near the center pier. The north and

south main spans of the bridge both showed numerous lateral cracks in the mid-span, and the north span was selected for the load test. The test sections of the bridge are shown in Figure 2. Section 1-1 is located at the mid-span of the bridge structure, Section 2-2 is at the location of the maximum positive bending moment in the side span, and Section 3-3 is located near the maximum negative bending moment at the center pier.
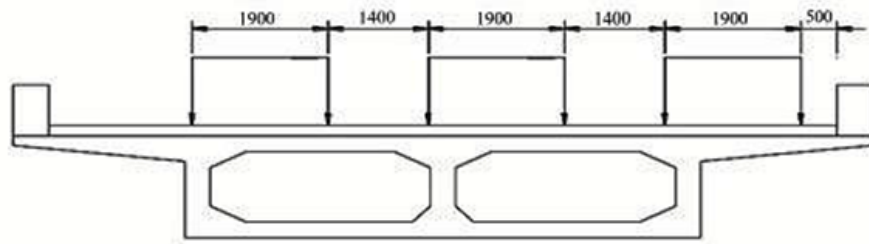


**Figure 3.** Transverse loading layout of vehicles (Unit: mm)



(a)



(b)



(c)
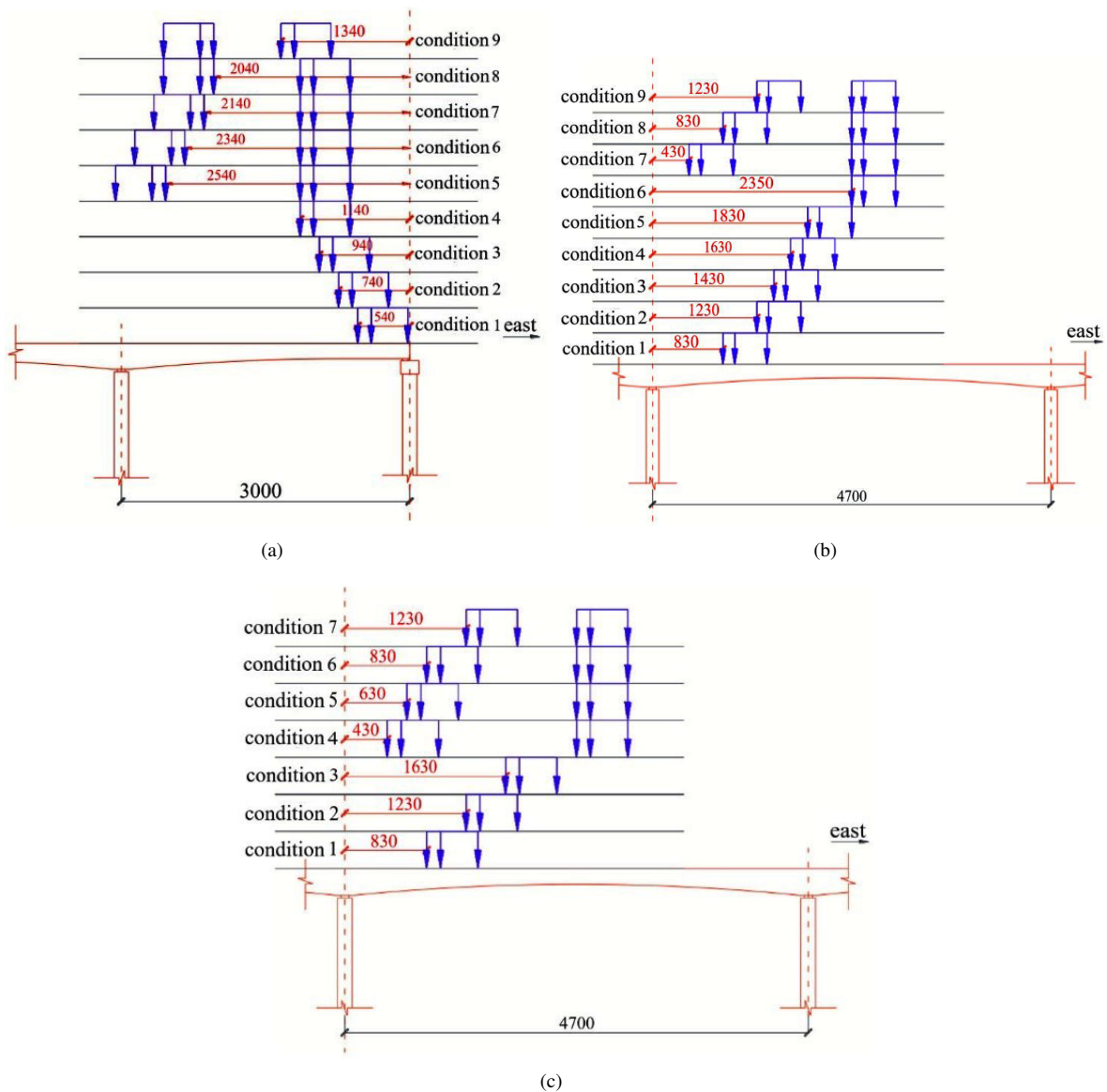
**Figure 4.** Longitudinal loading position diagrams (a) Section 2-2 (b) Section 1-1 (c) Section 3-3 (Unit: cm)

In the static load test, six three-axle heavy trucks were used, with each vehicle having a total weight of approximately 36 tons. The wheelbase between the front axle and middle axle is 3.8m, and between the middle axle and rear axle is 1.4m, with a lateral wheel spacing of 1.9m. The transverse loading positions at each test section are

3

shown in Figure 3. The loading conditions for the maximum positive bending moment in the side span (Section 2-2) are illustrated in subgraph (a) of Figure 4, the loading conditions for the maximum positive bending moment in the middle span (Section 1-1) are shown in subgraph (b) of Figure 4, and the loading conditions for the maximum negative bending moment near the center pier (Section 3-3) are shown in subgraph (c) of Figure 4.

## 3  Results and Discussion

The loading vehicles were applied according to the sequence shown in Figure 4. During the loading process for the maximum positive bending moment condition in the side span, the strain verification coefficient at point 2-1# increased continuously, and by the 6th level of loading, the verification coefficient reached 1.15, exceeding the limit value of 1.0 according to the standard. Loading was stopped at this point, as further loading could cause cracking in the bottom slab of the side span box girder. Due to the extensive lateral cracks at the bottom of the middle span, loading at Sections 1-1 and 2-2 was stopped after reaching 1.03 times or 0.97 times the highway Grade II load, respectively. At Section 1-1, the strain verification coefficient reached 2.53 when the maximum load level was applied, far exceeding the standard requirements. Table 1 shows the measured and theoretical strain results for the reinforcement, with only the strain results for Section 2-2 listed as the loading arrangement at Section 3-3 is identical to that at Section 2-2.

**Table 1.** Measured and theoretical strain results of reinforcement

| Key Measurement Point | Load Level | Measured Reinforcement Strain ($\mu\varepsilon$) | Theoretical Reinforcement Strain ($\mu\varepsilon$) | Measured Strain / Theoretical Strain | Load Efficiency (%) |
|---|---|---|---|---|---|
| 1-1 Section 1-1# Measurement Point | 1 | 47.5 | 21.3 | 2.23 | 0.2 |
| | 2 | 66.7 | 34.2 | 1.95 | 0.32 |
| | 3 | 93.3 | 42 | 2.22 | 0.39 |
| | 4 | 114.2 | 50.9 | 2.24 | 0.48 |
| | 5 | 148.4 | 60.7 | 2.44 | 0.57 |
| | 6 | 179.2 | 70.3 | 2.55 | 0.66 |
| | 7 | 206.7 | 81.6 | 2.53 | 0.77 |
| 2-2 Section 2-1# Measurement Point | 1 | 9.2 | 15.3 | 0.6 | 0.18 |
| | 2 | 19.2 | 25.6 | 0.75 | 0.29 |
| | 3 | 31.7 | 36 | 0.88 | 0.42 |
| | 4 | 13.3 | 47 | 0.92 | 0.54 |
| | 5 | 56.7 | 56.3 | 1.01 | 0.65 |
| | 6 | 72.5 | 63.1 | 1.15 | 0.73 |

**Table 2.** Strain data and verification coefficient results for each test location

| Test Section | Load Condition | Measurement Point Position | Point Number | Measured Strain ($\mu\varepsilon$) | Theoretical Strain ($\mu\varepsilon$) | Measured Strain / Theoretical Strain |
|---|---|---|---|---|---|---|
| 1-1 | Mid-span | Bottom Slab Reinforcement | 1-1# | 206.7 | 81.6 | 2.53 |
| | | | 1-2# | 66.7 | 79.3 | 0.84 |
| | | | 1-3# | 113.4 | 77.5 | 1.46 |
| 2-2 | Maximum Positive Bending Moment at Side Span | Bottom Slab Reinforcement | 2-1# | 72.5 | 63.1 | 1.15 |
| | | Slab concrete | 2-7# | / | 61.3 | / |
| | | | 2-8# | 40.9 | 60 | 0.68 |
| 3-3 | Near Center Pier | Flange reinforcement | 3-1# | 12.5 | 19.1 | 0.65 |
| | | Concrete surface | 3-2# | -34.6 | -32.1 | 1.08 |
| | | | 3-3# | -32.5 | -31.2 | 1.04 |
| | | | 3-4# | -33.9 | - 30.6 | 1.11 |
| | | | 3-5# | -24.5 | -25.3 | 0.97 |

Note: The strain gauge at point 2-7# in Table 2 was damaged during the test, and its data is not included in the analysis

Table 2 presents the strain data and verification coefficient results for various test locations. The strain gauge at point 2-7# in the 2-2 section was damaged during the test and is not considered in the data analysis. According to Table 2, under the test load, the verification coefficients for the strain measurement points 1-1# to 1-3# in the 1-1

section are 2.53, 0.84, and 1.46, respectively, with the verification coefficients for points 1-1# and 1-3# exceeding 1.0. For the 2-2 section, the verification coefficients for the strain measurement at 2-1# and the concrete strain at 2-3# are 1.15 and 0.68, respectively, with point 2-1# exceeding the limit of 1.0. At the 3-3 section, the strain verification coefficients for points 3-1# to 3-5# range from 0.65 to 1.11, with the verification coefficients for the bottom slab concrete strain measurement points ranging from 1.04 to 1.11, all exceeding 1.0. These strain test results clearly indicate that the load-bearing capacity of the continuous box girder no longer meets the requirements of the standards.

Due to the presence of numerous transverse cracks in the bottom of the box girder, the section stiffness is reduced after the concrete cracks. During the inspection, some areas of the box girder were found to have holes, which may have been caused by insufficient vibration during the construction process. Both the cracking of the box girder section and the presence of holes due to insufficient concrete vibration lead to section weakening. To estimate the current section weakening of the bridge, this analysis of the box girder damage is based on the measured results from the pre-reinforcement load test.

## 4 Damage Analysis of the Box Girder

Based on the load test, when the 1-1 section reached the 7th load level, the measured deflection at the mid-span control section was 11.76 mm. A finite element model of vehicle loading was established on the basis of the bridge's finite element analysis model, and the vehicle load positions for levels 1 to 7 were applied as per the actual layout.

The box girder verification was conducted using the general-purpose finite element analysis software Midas Civil 2023. A spatial beam model was created for the bridge's calculation and analysis. The deflection at the mid-span control section of the box girder was found to be 11.2 mm (Figure 5), which is less than the measured deflection. Therefore, the section stiffness of the box girder was reduced. When the section reduction reached 5%, the calculation results, shown in Figure 6, yielded a mid-span control section deflection of 11.7 mm, which is in close agreement with the actual measured value. Thus, the section weakening degree is estimated to be 5%.
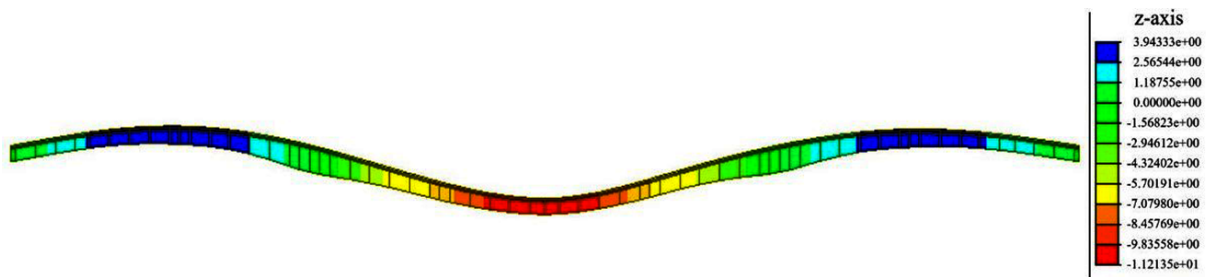


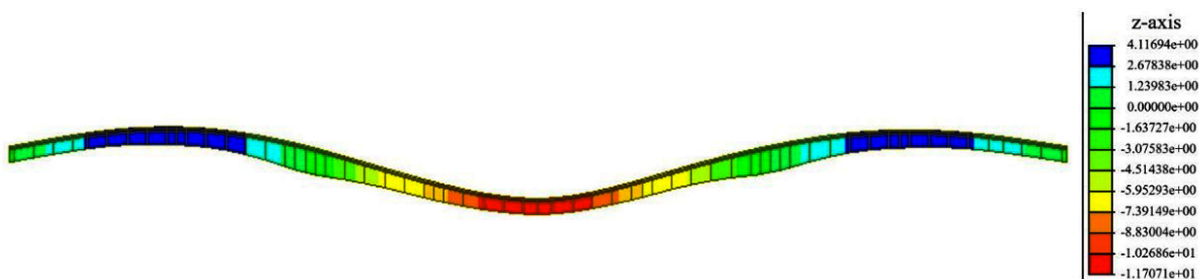**Figure 5.** Deflection results with section weakening (Unit: mm)



**Figure 6.** Deflection results with 5% section weakening simulation (Unit: mm)

**Table 3.** Prestress loss analysis models

| Model | Section Weakening | Additional Prestress Loss | Load Level |
|---|---|---|---|
| Model 1 | / | 0 | Highway Class I |
| Model 2 | / | 10 % | Highway Class I |
| Model 3 | 5 % | 10 % | Highway Class I |
| Model 4 | 5 % | 20 % | Highway Class I |

**Table 4.** Theoretical calculation results for four models

| Condition | Model 1 Mid-span | Model 2 Mid-span | Model 3 Mid-span | Model 4 Mid-span |
|---|---|---|---|---|
| Internal Force (kN · m) | 48931 | 48921 | 47909 | 46867 |
| Resistance (kN · m) | 49463 | 49143 | 49143 | 49143 |
| Margin (%) | 1.08% | 0.45% | 2.51% | 4.63% |
| Bottom Stress (MPa) | -1.305 | -1.54 | -2.36 | -3.22 |

Given the stress-induced cracks in the box girder, an additional consideration of prestress loss is taken into account. The calculated results are compared with the current state of the bridge to estimate the actual prestress in the original prestressing tendons after years of use and the cracking of the girder. Models with different levels of prestress loss were established, as shown in Table 3.

Based on the analysis above, four different prestress loss analysis models were established. The calculation results are summarized in Table 4, which lists the resistance and stress results at the bottom of the box girder.

From the calculation results in Table 4, it can be observed that the original mid-span resistance of the main girder has less than 5% reserve capacity. As a result of repeated vehicle loads, concrete shrinkage and creep, carbonation cracking, prestress loss, and other factors, when the section stiffness is reduced by 5% and the prestress loss reaches 10%, transverse cracks appear at the bottom of the main girder. This is consistent with the results from the actual bridge inspection. Therefore, the analysis and calculation of the box girder are performed considering a 5% section stiffness reduction and 10% prestress loss.

## 5 Conclusion

In this chapter, the damaged box girder was analyzed through pre-reinforcement load tests, and a finite element analysis model was established to determine the extent of section stiffness degradation and prestress loss. The main tasks undertaken are as follows:

(1) Load Test Results: Through the pre-reinforcement load test, it was found that the strain verification coefficients at the measurement points on the control sections ranged from 0.65 to 2.53, while the deflection verification coefficients ranged from 0.89 to 1.03. Most of the verification coefficients exceeded the threshold value of 1.0, indicating that the box girder structure failed to meet the code requirements.

(2) Section Stiffness Degradation: The section stiffness of the box girder was reduced, and when the section was weakened by 5%, the mid-span deflection at the control section of the box girder was calculated to be 11.7 mm, which was in good agreement with the actual measurements. Therefore, the analysis was conducted considering a 5% section stiffness reduction.

(3) Prestress Loss Analysis: The additional prestress loss of the box girder was analyzed. When the prestress loss reached 10%, transverse cracks appeared at the bottom of the main girder, which was consistent with the results from the actual bridge inspection. Therefore, the analysis and calculation were carried out with a 10% prestress loss in the box girder.

**Data Availability**

The data used to support the findings of this study are available from the corresponding author upon request.

**Conflicts of Interest**

The author declare that they have no conflicts of interest.

**References**

[1] Ministry of Transport of the People's Republic of China Website, "2023 statistical bulletin on the development of the transportation industry," *J. Waterw. Harb.*, vol. 45, no. 3, p. 308, 2023. https://doi.org/10.3969/j.issn.1005-8443.2024.03.001

[2] Z. L. Li, "Common defects and maintenance methods for roads and bridges," *Create Living*, vol. 2024, no. 8, pp. 52–54, 2024. https://doi.org/10.3969/j.issn.2095-4085.2024.08.019

[3] L. J. Wang, "An analysis of the application of external prestressing technology in the reinforcement of continuous rigid frame bridges," *Transpo World*, vol. 2024, no. 23, pp. 149–151, 2024. https://doi.org/10.3969/j.issn.1006-8872(s).2024.23.049

[4] F. A. Fathelbab, M. S. Ramadan, and A. Al-Tantawy, "Strengthening of RC bridge slabs using CFRP sheets," *Alex. Eng. J.*, vol. 53, no. 4, pp. 843–854, 2014. https://doi.org/10.1016/j.aej.2014.09.010

[5] J. D. Guo, "Research on external prestressed cable reinforcement of continuous beam bridges," *Eng. Technol. Res.*, vol. 9, no. 3, pp. 68–70, 2024. https://doi.org/10.19537/j.cnki.2096-2789.2024.03.023

[6] M. Xu, Z. Liu, X. Liu, W. Wang, L. Wang, and Z. Shi, "Investigation on interfacial shear performance of concrete strengthened with bonded steel plate," *J. Build. Eng.*, vol. 82, p. 108343, 2024. https://doi.org/10.1016/j.jobe.2023.108343

[7] K. D. Raithby, "Strengthening of concrete bridge decks with epoxy-bonded steel plates," *Int. J. Adhes. Adhes.*, vol. 2, no. 2, pp. 115–118, 1982. https://doi.org/10.1016/0143-7496(82)90124-5

[8] R. N. Swamy, R. Jones, and J. W. Bloxham, "Structural behaviour of reinforced concrete beams strengthened by epoxy bonded steel plates," *Struct. Eng.*, vol. 65, no. 2, pp. 59–68, 1987.

[9] D. J. Oehlers, M. M. Ali, and W. Luo, "Upgrading continuous reinforced concrete beams by gluing steel plates to their tension faces," *J. Struct. Eng.*, vol. 124, no. 3, pp. 224–232, 1998. https://doi.org/10.1061/(ASCE)0733-9445(1998)124:3(224)

[10] M. Hussain, A. Sharif, I. B. M. Baluch, and G. J. Al-Sulaimani, "Flexural behavior of precracked reinforced concrete beams strengthened externally by steel plates," *Struct. J.*, vol. 92, no. 1, pp. 14–23, 1995. https://doi.org/10.14359/1466

[11] Y. Q. Xiang, G. B. Tang, and C. X. Liu, "Cracking mechanism and simplified design method for bottom flange in prestressed concrete box girder bridge," *J. Bridge Eng.*, vol. 16, no. 2, pp. 267–274, 2011. https://doi.org/10.1061/(ASCE)BE.1943-5592.0000151

[12] S. X. Yu, "Analysis and prevention of cracks in prestressed concrete continuous box girders," *Transpo World*, vol. 2018, no. 9, pp. 88–89, 2018.

[13] X. S. Xiao, "Analysis and preventive measures for cracks in prestressed concrete continuous box girders," *Green Environ. Friendly Build. Mater.*, vol. 2017, no. 6, p. 127, 2017.

[14] A. C. Aparicio and G. Ramos, "Flexural strength of externally prestressed concrete bridges," *Struct. J.*, vol. 93, no. 5, pp. 512–523, 1996. https://doi.org/10.14359/9709

[15] K. H. Tan and C. K. Ng, "Effects of deviators and tendon configuration on behavior of externally prestressed beams," *Struct. J.*, vol. 94, no. 1, pp. 13–22, 1997. https://doi.org/10.14359/456

[16] Z. P. Bažant, "Prediction of concrete creep and shrinkage: Past, present and future," *Nucl. Eng. Des.*, vol. 203, no. 1, pp. 27–38, 2001. https://doi.org/10.1016/S0029-5493(00)00299-5

[17] M. Harajli, N. Khairallah, and H. Nassif, "Externally prestressed members: Evaluation of second-order effects," *J. Struct. Eng.*, vol. 125, no. 10, pp. 1151–1161, 1999. https://doi.org/10.1061/(ASCE)0733-9445(1999)125:10(1151)

[18] Y. L. Wang, J. S. Zhu, S. Y. Jia, and M. Akiyama, "Time-dependent deflection prediction of long-span prestressed concrete bridges considering the environmental effects," *Eng. Struct.*, vol. 322, p. 119163, 2025. https://doi.org/10.1016/j.engstruct.2024.119163

[19] Y. H. Park, C. Park, and Y. G. Park, "The behavior of an in-service plate girder bridge strengthened with external prestressing tendons," *Eng. Struct.*, vol. 27, no. 3, pp. 379–386, 2005. https://doi.org/10.1016/j.engstruct.2004.10.014

[20] A. H. Ghallab, M. A. Khafaga, M. F. Farouk, and A. Essawy, "Shear behavior of concrete beams externally prestressed with Parafil ropes," *Ain Shams Eng. J.*, vol. 4, no. 1, pp. 1–16, 2013. https://doi.org/10.1016/j.asej.2012.05.003

[21] F. Peng, W. Xue, and Y. Tan, "Design approach for flexural capacity of prestressed concrete beams with external tendons," *J. Struct. Eng.*, vol. 144, no. 12, p. 04018215, 2018. https://doi.org/10.1061/(ASCE)ST.1943-541X.0002208

[22] W. Xue, Y. Tan, and F. Peng, "Experimental study on damaged prestressed concrete beams using external post-tensioned tendons," *ACI Struct. J.*, vol. 117, no. 1, p. 159, 2020. https://doi.org/10.14359/51718019

[23] Z. B. Huang, Q. Z. Luo, and Y. J. Wu, "Deflection analysis and external prestressing reinforcement evaluation of continuous box-girder bridge," *J. Water Resour. Archit. Eng.*, vol. 14, no. 5, pp. 75–79, 2016. https://doi.org/10.3969/j.issn.1672-1144.2016.05.014

[24] H. Liu, F. X. Zeng, and X. B. Cao, "Disease analysis and external prestressed reinforcement of a PC continuous box girder bridge," *Shanxi Archit.*, vol. 45, no. 22, pp. 124–125, 2019. https://doi.org/10.3969/j.issn.1009-6825.2019.22.058